

# In Situ Infrared Study of Water–Sulfate Coadsorption on Gold(111) in Sulfuric Acid Solutions

Ken-ichi Ataka and Masatoshi Osawa\*

Catalysis Research Center, Hokkaido University, Sapporo 060, Japan

Received October 10, 1997. In Final Form: December 8, 1997

Potential-dependent reorientation of a water molecule, adsorption of sulfate, and interactions between water and sulfate on a highly ordered Au(111) electrode surface in sulfuric acid solutions have been investigated in situ as a function of applied potential by means of surface-enhanced infrared absorption spectroscopy. The spectrum of the water layer at the interface changes in both intensity and frequency as the applied potential changes due to the reorientation of water molecules. The orientations deduced from infrared spectra are in good agreement with the predictions made by molecular dynamics simulations at potentials below and around the potential of zero charge (pzc) of the electrode where sulfate adsorption is negligible. At potentials above the pzc, sulfate anion is adsorbed at 3-fold hollow sites on the (111) surface via three oxygen atoms. When the potential is increased and the fractional coverage of sulfate reaches to about one-half of full coverage, adsorbed sulfate anions start to form short-ranged domains and greatly change the water layer structure. Water molecules stabilize the sulfate domains by bridging neighboring sulfate anions via hydrogen bonding. The weak tunneling spots observed in the reported scanning tunneling microscopy images of the well-ordered ( $\sqrt{3} \times \sqrt{7}$ ) sulfate adlayers on (111) metal surfaces are attributed to water molecules that bridge adjacent adsorbed sulfate anions.

## Introduction

Understanding the composition, structure, and properties of solid/liquid interfaces is one of the most important subjects in electrochemistry.<sup>1,2</sup> The recent development of in situ microscopic level techniques, including scanning tunneling microscopy (STM) and infrared (IR) spectroscopy, has facilitated detailed studies of the interfaces on the atomic and molecular scales.<sup>3,4</sup> In this paper, an in situ IR study of water molecules and anions at a highly ordered Au(111) surface in sulfuric acid solutions is reported.

This study was stimulated by recent STM studies of the specific anion adsorption on well-ordered (111) surfaces of Au, Rh, and Pt in sulfuric acid solutions.<sup>5–8</sup> Magnussen et al.<sup>5</sup> first found that adsorbed anions form an ordered structure with a ( $\sqrt{3} \times \sqrt{7}$ ) symmetry on Au(111) at high potentials in the double-layer region. Almost identical ordered structures have been observed on the (111) surfaces of Rh<sup>7</sup> and Pt<sup>8</sup> also. However, the interpretations of the observed STM images are controversial. The controversy arises from an additional weak tunneling spot observed in the unit cell. The additional spot is observed either near the center of the unit cell or at a position between main bright spots along the  $\sqrt{7}$  direction depending upon imaging conditions. Magnussen et al.<sup>5</sup>

attributed all the tunneling spots to bisulfate ( $\text{HSO}_4^-$ ) with coverage of 0.4. However, Shi et al.<sup>9</sup> showed by chronocoulometry and radiochemical assay that sulfate ( $\text{SO}_4^{2-}$ ) is predominant adsorbate rather than bisulfate even in very strong acidic solutions. More important is that its maximum coverage is 0.2. On the basis of these findings, Edens et al.<sup>6</sup> attributed the bright spots to adsorbed sulfate anions and the weak spots to hydronium (oxonium) cations ( $\text{H}_3\text{O}^+$ ) incorporated in the sulfate adlayer. Nevertheless, no evidence of the hydronium coadsorption has been obtained. On the other hand, Wan et al.<sup>7</sup> attributed the weak spots to water molecules forming one-dimensional icelike chains extending along the  $\sqrt{3}$  direction. Very recently, Funtikov et al.<sup>8</sup> also concluded that water molecules are coadsorbed in the sulfate adlayer on Pt(111). The last authors suggested that hydrogen bonding between water and sulfate is responsible for the ordering of adsorbed sulfate anions.<sup>8</sup>

Coadsorption of water and ionic species on metal surfaces has extensively been studied in ultrahigh vacuum (UHV) as a model of the electrochemical interface, and it has been found that ionic species stabilize water layer via hydrogen bonding or other mechanisms.<sup>10–12</sup> However, in situ studies of water–ion interactions at the electrochemical interface have been limited and very little is known. In a previous in situ IR study of a Au(111)-like electrode surface, we found that specific anion adsorption significantly changes the interfacial structure.<sup>13</sup> Hydrophobic anions such as perchlorate and chloride disrupt hydrogen bonds between interfacial water molecules, whereas hydrophilic anions such as sulfate form hydrogen bonds with water molecules. In the present study, interactions between water and sulfate at the electro-

\* To whom correspondence may be addressed: phone +81-11-706-2909; fax, +81-11-709-4748; e-mail, osawam@cat.hokudai.ac.jp.

(1) Delahay, P. *Double Layer and Electrode Kinetics*; Interscience Publishers: New York, 1965.

(2) Bockris, J. O'M.; Khan, S. U. M. *Surface Electrochemistry: A Molecular Level Approach*; Plenum: New York, 1993.

(3) Lipkowski, J.; Ross, P. N., Eds. *Adsorption of Molecules at Metal Electrodes*; VCH: New York, 1992.

(4) Lipkowski, J.; Ross, P. H., Eds. *Structure of Electrified Interfaces*; VCH: New York, 1993.

(5) Magnussen, O. M.; Hangebock, J.; Hotlos, J.; Behm, R. J. *Faraday Discuss.* **1992**, *94*, 329.

(6) Edens, G. J.; Gao, X.; Weaver, M. J. *Electroanal. Chem.* **1994**, *375*, 357.

(7) Wan, L.-J.; Yau, S.-L.; Itaya, K. *J. Phys. Chem.* **1995**, *99*, 9507.

(8) Funtikov, A. M.; Stimming, U.; Vogel, R. *J. Electroanal. Chem.* **1997**, *428*, 147.

(9) Shi, Z.; Lipkowski, J.; Gamboa, M.; Zelenay, P.; Wieckowski, A. *J. Electroanal. Chem.* **1994**, *366*, 317.

(10) Thiel, P. A.; Madey, T. E. *Surf. Sci. Rep.* **1987**, *7*, 211.

(11) Bange, K.; Grider, D. E.; Madey, T. E.; Sass, J. K. *Surf. Sci.* **1984**, *136*, 38.

(12) Krasnopoler, A.; Stuve, E. M. *Surf. Sci.* **1994**, *303*, 355.

(13) Ataka, K.; Yotsuyanagi, T.; Osawa, M. *J. Phys. Chem.* **1996**, *100*, 10664.

chemical interface are discussed in more detail in connection with the published STM data.

In the most previous *in situ* IR studies of the electrochemical interface, the so-called reflection-absorption spectroscopy (RAS) technique has been used.<sup>14</sup> In these measurements, IR radiation is passed through the solution phase with a thickness of a few micrometers. Therefore, signals from the interface (the inner part of the double layer with a thickness of  $\sim 1$  nm) are superposed on the several orders of magnitude larger solution background. It is very difficult to completely subtract the solution background even if a difference of spectra collected at two different suitable potentials is measured. The question always arises in this type of measurement as to whether the observed bands are attributed to the species at the interface or in the bulk solution. To avoid this problem, a surface-enhanced IR absorption spectroscopy (SEIRAS) technique combined with attenuated-total-reflection (ATR) technique<sup>15</sup> was used in the present study instead of RAS because ATR-SEIRAS is more surface sensitive than RAS. In ATR-SEIRAS measurements, a very thin metal film evaporated on an IR transparent prism is used as the working electrode. IR radiation is focused at the electrode surface by being passed through the prism and the radiation totally reflected at the interface is measured. The use of the ATR configuration significantly reduces the solution background. Furthermore, the use of the very thin film electrode greatly enhances the signals from the very near vicinity of the electrode surface via the excitation of localized plasmon resonance of the metal.<sup>16</sup> Solution background is comparable to the signals from the interface in ATR-SEIRAS measurements and can be subtracted very successfully by taking a potential difference.<sup>15</sup> Vibrational modes that have dipole changes normal to the surface are selectively enhanced in SEIRAS as in the case of RAS.<sup>16</sup> This surface selection rule is useful to determine orientations of adsorbed species.

## Experimental Section

Experimental procedures and the electrochemical cell used were the same as those reported in our previous papers.<sup>13,15</sup> Briefly, a 20 nm thick Au film, evaporated on a hemicylindrical Si prism (1 cm in radius and 2.5 cm in length) under a vacuum of  $5 \times 10^{-5}$  Pa, was used as the working electrode. The thickness of the metal film was monitored and controlled by a quartz crystal microbalance. The deposition rate was kept to 0.01 nm/s during the evaporation. The electrode surface was cleaned in the test solution by cycling the potential between a potential slightly positive to hydrogen evolution and a potential slightly negative to oxygen evolution. All the potentials are quoted versus the reversible hydrogen electrode (RHE) in the same solution. The counter electrode was a Au foil.

The electrolyte solutions were prepared from suprapur sulfuric acid (Merk) and ultrapure Millipore water, which were deaerated with argon before the experiments.

The Fourier-transform IR spectrometer used was a Bio-Rad FTS 60A/896 equipped with a linearized high-sensitivity HgCdTe detector (Bio-Rad). The spectrometer was operated at a resolution of  $4 \text{ cm}^{-1}$ . Spectra were acquired during a potential sweep at a rate of 5 mV/s by using a software supplied by Bio-Rad (KINETICS). Sixty four interferograms were averaged for each spectrum to enhance the signal-to-noise ratio. The acquisition time is ca. 10 s per spectrum; hence each spectrum is the average of every 50 mV interval. Spectra are shown in the absorbance

units defined as  $-\log(I/I_0)$ , where  $I$  and  $I_0$  represent the intensities of signals at the sample and reference potentials, respectively.

In the present study, we employed a two-dimensional (2D) IR technique<sup>17</sup> to accentuate certain useful information that is not distinctly seen in usual one-dimensional spectra. The basic concept of 2D IR is somewhat analogous to that of the 2D correlation technique used in NMR. Through the 2D correlation analysis of a series of potential-dependent spectra, IR signals arising from different species can be clearly distinguished by their characteristic potential-dependent behavior.

The 2D correlation analysis was carried out with the generalized 2D IR formalism proposed by Noda.<sup>17</sup> Given a spectral variation at wavenumber  $\nu$  observed for a period of time  $t$  between  $-T/2$  and  $T/2$ ,  $y(\nu, t)$ , the dynamic spectrum,  $\bar{y}(\nu, t)$ , is defined as

$$\bar{y}(\nu, t) = \begin{cases} y(\nu, t) - \bar{y}(\nu) & \text{for } -T/2 \leq t \leq T/2 \\ 0 & \text{otherwise} \end{cases} \quad (1)$$

where  $\bar{y}(\nu)$  is the time-average spectrum

$$\bar{y}(\nu) = \frac{1}{T} \int_{-T/2}^{T/2} y(\nu, t) dt \quad (2)$$

The correlation intensity between two arbitrary wavenumbers,  $\nu_1$  and  $\nu_2$ , is defined as

$$\Phi(\nu_1, \nu_2) + i\Psi(\nu_1, \nu_2) = \frac{1}{\pi T} \int_0^\infty \bar{Y}_1(\omega) \cdot \bar{Y}_2^*(\omega) d\omega \quad (3)$$

where

$$\bar{Y}_1(\omega) = \int_{-\infty}^\infty \bar{y}(\nu_1, t) e^{-i\omega t} dt \quad (4)$$

$$\bar{Y}_2^*(\omega) = \int_{-\infty}^\infty \bar{y}(\nu_2, t) e^{+i\omega t} dt \quad (5)$$

It is noted that *time* can be replaced by *potential* since the spectral collections are carried out during a linear potential sweep.

The real and imaginary components of the correlation function,  $\Phi(\nu_1, \nu_2)$  and  $\Psi(\nu_1, \nu_2)$ , are plotted over a spectral plane defined by the two independent wavenumber axes,  $\nu_1$  and  $\nu_2$ , which are referred to, respectively, as the synchronous and asynchronous spectra. The synchronous spectrum characterizes the coherence of dynamic fluctuation of IR signals measured at two different wavenumbers. If the variations of the two IR signals are similar to each other, peaks appear at coordinates  $(\nu_1, \nu_2)$  and  $(\nu_2, \nu_1)$  in the synchronous spectrum. On the other hand, the asynchronous spectrum is complementary to the synchronous spectrum and characterizes the independent fluctuations of IR signals. Peaks appear in the asynchronous spectrum if the IR signals vary at different rates and/or phases.

## Results and Discussion

### Morphology of Evaporated Thin Au Electrode.

The evaporated thin Au electrode used in both electrochemical and IR measurements consisted of islands (particles) of 50–80 nm in diameter. The island structure facilitates the excitation of localized plasmon of the metal and plays a key role in the IR absorption enhancement for species in the very near vicinity of the metal surface.<sup>16</sup> A typical STM image of the electrode is shown in Figure 1. The figure shows that the surfaces of the islands are constructed with wide terraces and steps. The angle of the terrace corners is roughly  $60^\circ$  or  $120^\circ$ , suggesting that the terraces are (111) single crystal planes.

**Cyclic Voltammogram.** Despite the island nature, conductivity of the metal film was high enough and no problems were found in electrochemistry. Figure 2 shows a cyclic voltammogram of the evaporated Au thin film electrode recorded in 0.1 M  $\text{H}_2\text{SO}_4$  at a sweep rate of 50 mV/s. The voltammogram is very similar to that of a well-

(14) For example, Nichols, R. J. In *Adsorption of Molecules at Metal Electrodes*; Lipkowski, J., Ross, P. N., Eds.; VCH: New York, 1992; p 347.

(15) Osawa, M.; Ataka, K.; Yoshii, K.; Yotsuyanagi, T. *J. Electron Spectrosc. Relat. Phenom.* **1993**, 64/65, 371.

(16) Osawa, M.; Ataka, K.; Yoshii, K.; Nishikawa, Y. *Appl. Spectrosc.* **1993**, 47, 1497.

(17) Noda, I. *Appl. Spectrosc.* **1993**, 47, 1329.

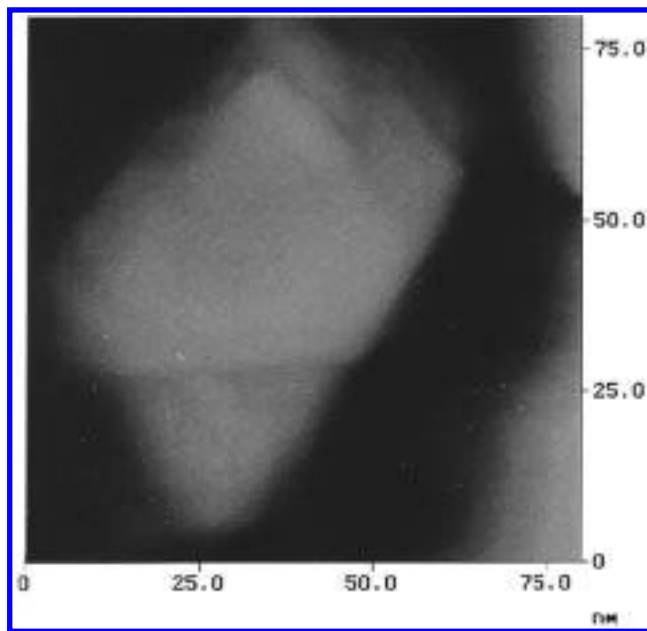


**Figure 1.** STM image of a Au thin film electrode evaporated on a Si prism.

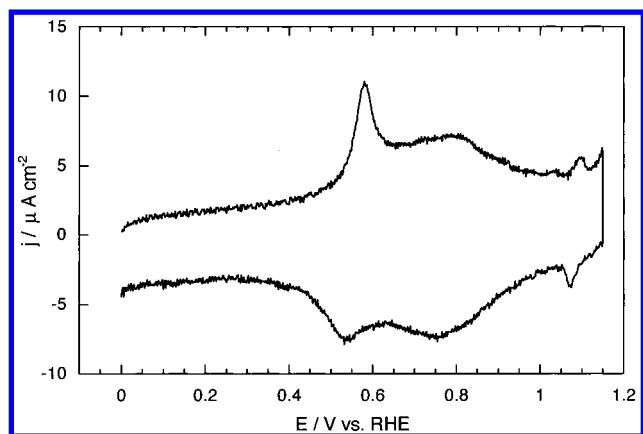


**Figure 2.** Cyclic voltammogram of Au electrode in 0.1 M H<sub>2</sub>SO<sub>4</sub>. Sweep rate is 50 mV/s.

defined Au(111) single-crystal surface.<sup>9,18,19</sup> The broad wave ranging from 0.5 and 1.0 V corresponds to the adsorption of sulfate. The current spike seen at 0.58 V has been ascribed to the lifting of the (1 × 23) reconstruction of the (111) surface to unreconstructed (1 × 1) phase.<sup>20</sup> Reversible sharp current spikes at 1.1 V is ascribed to the disorder–ordered transition of the sulfate adlayer.<sup>5,6</sup> These current spikes are characteristic for highly ordered Au(111) surfaces. However, the relatively weak intensity of the disorder–order transition spike indicates the presence of defect sites on the (111) surface.<sup>21</sup>

**IR Spectra of the Interface.** A series of IR spectra collected during a potential sweep from 0.0 to 1.2 V are shown in Figure 3. A single beam spectrum collected at 0.0 V prior to the potential-sweep experiment was used as the reference. The reference potential was chosen in view of the negligible anion adsorption. The negative- and positive-going bands around 3500 and 1650 cm<sup>-1</sup> are

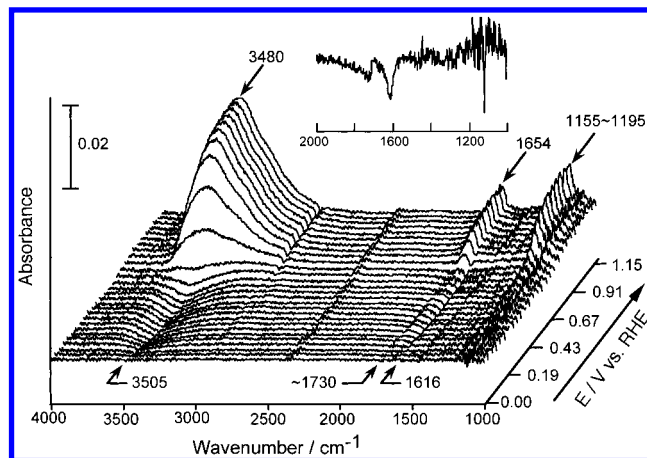


**Figure 3.** 3-D perspective plot showing the IR spectra of the interface as a function of the applied potential. Spectra were obtained during a potential sweep from 0.0 to 1.2 V at 5 mV/s. The spectrum acquired at 0.0 V was used as the reference. The inset shows the spectrum at 0.48 V.

assigned to the OH stretching ( $\nu$ ) and HOH bending ( $\delta$ ) modes, respectively, of water. The negative (positive) sign indicates that the intensity decreases (increases) with respect to the reference spectrum. Remarkable changes are evident around 0.5 V for the water bands. The sign of the bands is negative at potentials below 0.5 V and is positive at potentials above 0.8 V, indicating that the intensities of the water bands decrease with increasing the potential up to about 0.5 V and then increase. Associated with the change in intensity, the  $\nu(\text{OH})$  band shifts from 3505 to 3480 cm<sup>-1</sup> and the  $\delta(\text{HOH})$  band shifts from 1616 to 1654 cm<sup>-1</sup>. Note that the potential at which the spectral changes occur is very close to the potential of zero charge (pzc) of Au(111) (about 0.5 V vs RHE in a 0.05 M KClO<sub>4</sub> + 0.02 M HClO<sub>4</sub> + 5 mM K<sub>2</sub>SO<sub>4</sub>).<sup>9</sup> Curve fitting analysis of the spectra revealed that the negative intensity of the 1615-cm<sup>-1</sup> band remains constant at potentials above 0.53 V. Since the adsorption of sulfate anions at potentials above 0.5 V will remove some amount of water molecules from the interface, the constant negative intensity indicates that the intrinsic intensity of this band (and also the corresponding  $\nu(\text{OH})$  band at 3505 cm<sup>-1</sup>) decreases to nearly zero around 0.5 V. On the other hand, the positive-going 1654-cm<sup>-1</sup> band appears at about 0.75 V. These results imply that the water layer at the interface has no or very weak IR absorption around the pzc.

The negative-going weak band at about 1730 cm<sup>-1</sup> is assigned to the doubly degenerated  $\delta(\text{HOH})$  of hydronium cation (see below). The band at 1155–1195 cm<sup>-1</sup> that increases in intensity with increasing the potential has been assigned to a  $\nu(\text{SO})$  mode of sulfate anion adsorbed on the electrode surface.<sup>6</sup> Additional weak bands are also observed. The negative-going bands at about 2900 cm<sup>-1</sup> are undoubtedly assigned to  $\nu(\text{CH})$  modes of alkyl chains probably of hydrocarbon contaminants. A weak feature seen at 1100 cm<sup>-1</sup> (the lower frequency shoulder of the sulfate band) is assigned to a  $\nu(\text{Si-O})$  mode of Si oxide (of the prism). Due to the low transmittance of the prism, the signal-to-noise ratio is worse in the low-frequency region below 1200 cm<sup>-1</sup> than in the higher frequency region. The spectral region below 1000 cm<sup>-1</sup> was omitted from this figure because of very low signal-to-noise ratio. However, we will show later by means of 2D IR technique that a weak band is located at about 955 cm<sup>-1</sup> (Figure 9).

For comparison, transmission spectra of pure water and sulfuric acid solutions (0.1 and ~5 M), sandwiched between two CaF<sub>2</sub> windows, are shown in Figure 4. The asym-

(18) Angerstein-Kozłowska, H.; Conway, B. E.; Hamelin, A.; Stocicviciu, L. *Electrochim. Acta* **1986**, *31*, 1051.

(19) Angerstein-Kozłowska, H.; Conway, B. E.; Hamelin, A.; Stocicviciu, L. *J. Electroanal. Chem.* **1987**, *228*, 429.

(20) Kolb, D. M. In *Structure of Electrified Interface*; Lipkowsky, J., Ross, P. N., Eds.; VCH: New York, 1993; p 65.

(21) Dretschkow, T.; Wandlowski, T. *Ber. Bunsen-Ges. Phys. Chem.* **1997**, *101*, 749.

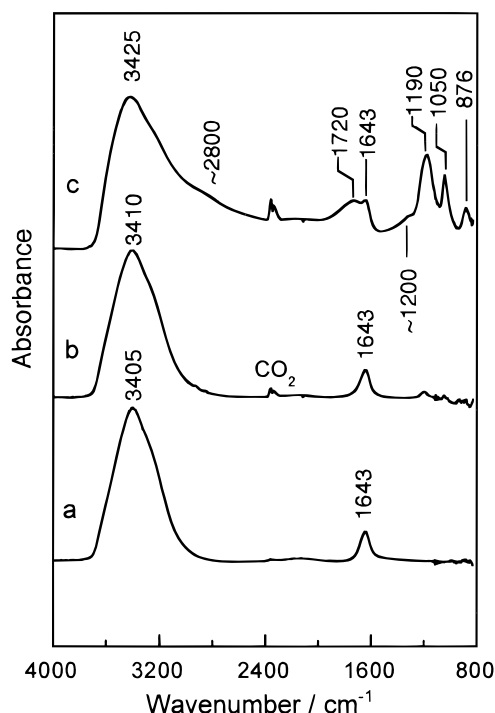


**Figure 4.** Transmission IR spectra of (a) pure water, (b) 0.1 M  $\text{H}_2\text{SO}_4$ , and (c)  $\sim 5$  M  $\text{H}_2\text{SO}_4$ .

metric and symmetric  $\nu(\text{SO})$  modes and  $\nu(\text{S}-\text{OH})$  mode of bisulfate anion are observed at 1190, 1050, and 876  $\text{cm}^{-1}$ , respectively. The broad bands around 2800, 1720, and 1200  $\text{cm}^{-1}$  are assigned, from higher to lower, to symmetric and/or asymmetric  $\nu(\text{OH})$ , doubly degenerate asymmetric  $\delta(\text{HOH})$ , and symmetric  $\delta(\text{HOH})$  of hydronium cation.<sup>22</sup> The spectra from the electrode surface shown in Figure 3 are different from those of the bulk solutions. The frequency of the water  $\nu(\text{OH})$  band in the surface spectra is higher than that in the bulk spectra, indicating weaker hydrogen bonding at the electrode surface. The  $\delta(\text{HOH})$  band is shifted to lower at low potentials and to higher at high potentials compared with that in the bulk spectra. Furthermore, the bands of bisulfate in bulk solution (1190 and 1050  $\text{cm}^{-1}$ ) are not observed in the surface spectra. Together with the potential-dependent spectral changes of both water and sulfate, it is concluded that the very near vicinity of the electrode surface was successfully observed without the interference from the bulk solution.

Almost the same spectra as shown in Figure 3 were obtained in a  $\text{Na}_2\text{SO}_4$  solution (pH = 5) in the present investigation. Since sulfate is predominant in the weakly acidic solution, the result strongly suggests that sulfate rather than bisulfate is adsorbed even in the strongly acidic solutions.

**Potential-Dependent Reorientation of Water at the Interface.** Electrochemical measurements predict that water molecules reorient from "oxygen-up" to "oxygen-down" as the electrode charge (or, equivalently, potential) changes from negative to positive.<sup>2</sup> The potential-dependent reorientation of water molecules at the electrochemical interface has been investigated in more detail by molecular dynamics simulations.<sup>23–25</sup> On the basis of the surface selection rule,<sup>16</sup> the potential-dependent

intensity changes of the water bands shown in Figure 3 is ascribed to the reorientation of water molecules. The absence of water bands around the pzc (about 0.5 V) implies that water molecules are lying parallel to the surface (Figure 5b). At potentials below and above the pzc, the oxygen-end of water becomes more oriented toward the surface or solution phase, resulting in the increase of the intensities.

Classical models of the electrochemical interface assume that the water molecule orients with its dipole directing toward the surface and interact with the surface via hydrogen atoms at potentials below the pzc.<sup>2</sup> However, the  $\nu(\text{OH})$  mode characteristic for the  $\text{OH}\cdots\text{metal}$  bonding is not observed in the expected region between 2935 and 2950  $\text{cm}^{-1}$ .<sup>10</sup> The negative-going bands observed around 2900  $\text{cm}^{-1}$  are too sharp to be assigned to the  $\nu(\text{OH})$  band. The  $\nu(\text{OH})$  band observed at potentials below the pzc is located at 3505  $\text{cm}^{-1}$ . This frequency is lower than that of free OH moiety (3600–3650  $\text{cm}^{-1}$ )<sup>10</sup> and the band shape is relatively broad, indicating weak hydrogen bonding. Nevertheless, the  $\delta(\text{HOH})$  mode is located in the very low frequency region for free or nearly free water molecules in the gas phase, noble gas matrixes, and organic solvents (1595–1630  $\text{cm}^{-1}$ ).<sup>26</sup> The unexpectedly low frequency of the  $\delta(\text{HOH})$  mode suggests an interaction of the oxygen lone-pair electron with the electrode surface.<sup>10</sup> The observed spectral features are explained by assuming that each water molecule is oriented with the two hydrogen atoms slightly closer to the electrode surface than the oxygen atom, as illustrated in Figure 5a. Note that the two hydrogen ends are free from hydrogen bonding because of the steric hindrance and only the lone-pair orbital directing toward the solution phase is available for hydrogen bonding with water molecules in the second layer. Thus the  $\nu(\text{OH})$  mode appears at the relatively high frequency.

Hydronium cation is coadsorbed on the electrode surface at potentials below 0.5 V, which is evident from the weak negative-going band at 1730  $\text{cm}^{-1}$  seen in Figure 3. The negative sign indicates that the intensity decreases as the potential is made more positive. The intensity change is that expected for cationic species. This band is assigned to doubly degenerate asymmetric  $\delta(\text{HOH})$  mode.<sup>22</sup> The corresponding symmetric  $\delta(\text{HOH})$  mode is not observed in the expected range around 1200  $\text{cm}^{-1}$ . To show the absence of the  $\delta(\text{HOH})$  mode more clearly, the 2000–1000  $\text{cm}^{-1}$  region of the spectrum at 0.48 V is shown in Figure 3 by vertically expanding. On the basis of the surface selection rule, the missing of the latter band is interpreted as the  $C_3$  axis of hydronium cation being oriented nearly parallel to the surface. Since water molecules are adsorbed on the electrode surface with hydrogen atoms slightly closer to the surface than the oxygen atoms, hydronium cation with the proposed orientation can be readily formed by adding the third proton to the lone-pair orbital of water directing toward the solution phase. Since hydronium cations diffuse in solutions and ice by proton hopping, the proposed orientation seems to be reasonable.

The spectral feature of the  $\nu(\text{OH})$  region is rather complicated at potentials between 0.5 and 0.8 V due to the overlap of the negative- and positive-going bands at 3505 and 3480  $\text{cm}^{-1}$ , respectively. We examined this potential range in detail by using the spectrum collected at 0.53 V as the reference. Since the intensity of the 3505-

(22) Nakamoto, K. *Infrared and Raman Spectra of Inorganic and Coordination Compounds*, 4th ed.; John Wiley & Sons: New York, 1986, and references therein.

(23) Nagy, G.; Heinzinger, K. *J. Electroanal. Chem.* **1990**, 296, 549.

(24) Nagy, G.; Heinzinger, K. *J. Electroanal. Chem.* **1992**, 327, 25.

(25) Heinzinger, K. In *Structure of Electrified Interface*; Lipkowski, J., Ross, P. N., Eds.; VCH: New York, 1993; p 239.

(26) Scherer, J. R. In *Advances in Infrared and Raman Spectroscopy*; Clark, R. J. H., Hester, R. E., Eds.; Heyden: Philadelphia, PA, 1978; Vol. 5, p 149.

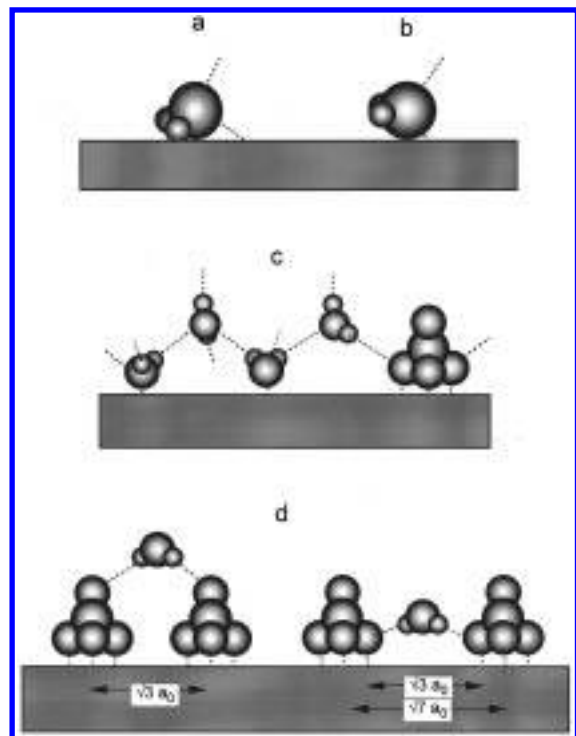


**Figure 5.** Orientations of water molecules on the Au(111) surface at potentials (a) below the pzc, (b) around the pzc, and (c) slightly above the pzc deduced from the IR spectra in Figure 3. The icelike structure (c) was taken from ref 10. Sulfate anions are adsorbed on the surface without disturbing the icelike structure when sulfate coverage is small. At higher potentials (d), water molecules bridge adjacent adsorbed sulfate anions separated by  $\sqrt{3}a_0$  and  $\sqrt{7}a_0$  ( $a_0$ , the nearest neighbor distance between surface metal atoms) via hydrogen bonding.

$\text{cm}^{-1}$  band decreases to nearly zero at about 0.53 V, this potential is suitable to remove the interference from this band. The result is shown in Figure 6, where it is seen that a very broad  $\nu(\text{OH})$  band appears around  $3200\text{ cm}^{-1}$  and grows in intensity as the potential is made more positive. The corresponding  $\delta(\text{HOH})$  band was too weak to be detected. One might have a doubt for the presence of the very weak band around  $3200\text{ cm}^{-1}$  since background subtraction sometimes yields artifacts. To confirm the presence of this band, we used a 2D IR technique. It is noted that 2D spectra are independent of the choice of the reference potential because the fluctuation of IR signals from the time (or potential) average is used for the correlation analysis (eq 1). The asynchronous 2D correlation spectrum constructed from the one-dimensional spectra collected during the potential sweep from 0 to 0.81 V (Figure 3) is shown in Figure 7. The potential-averaged one-dimensional spectrum is shown at the top and left sides of the 2D map for comparison. A set of cross peaks are seen at the coordinates (3505,  $\sim 3200$ ) and ( $\sim 3200$ , 3505). The cross peaks clearly demonstrate the presence of the very broad band at  $\sim 3200\text{ cm}^{-1}$  that changes intensity *independently* of the  $3505\text{-cm}^{-1}$  band. No cross peaks were observed in asynchronous 2D spectra constructed from the potential-dependent spectra collected below 0.6 V, indicating that the  $3200\text{-cm}^{-1}$  band appears at a potential above 0.6 V and grows in intensity with increasing potential. The 2D analysis is consistent with Figure 6.

The spectral feature of the interfacial water shown in Figure 6 is very similar to that of ice.<sup>22</sup> The presence of an icelike water layer at solid/liquid interfaces has been predicted by recent molecular dynamics simulations.<sup>23–25</sup>

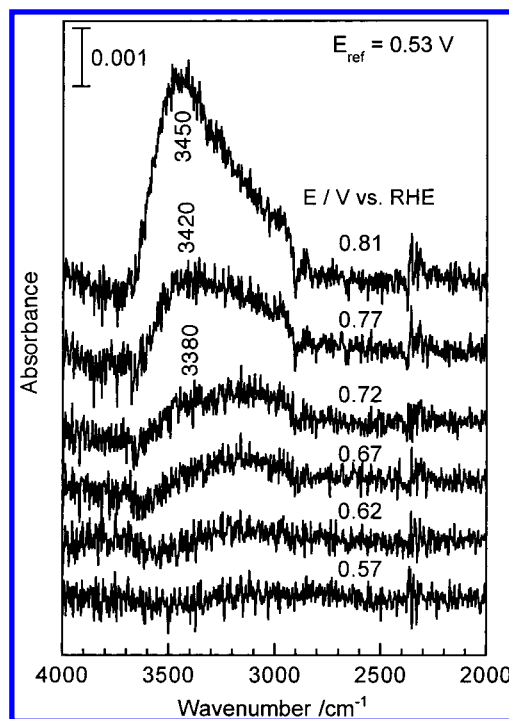


**Figure 6.** IR spectra of water at the electrode surface obtained by using a spectrum acquired at 0.53 V as the reference.

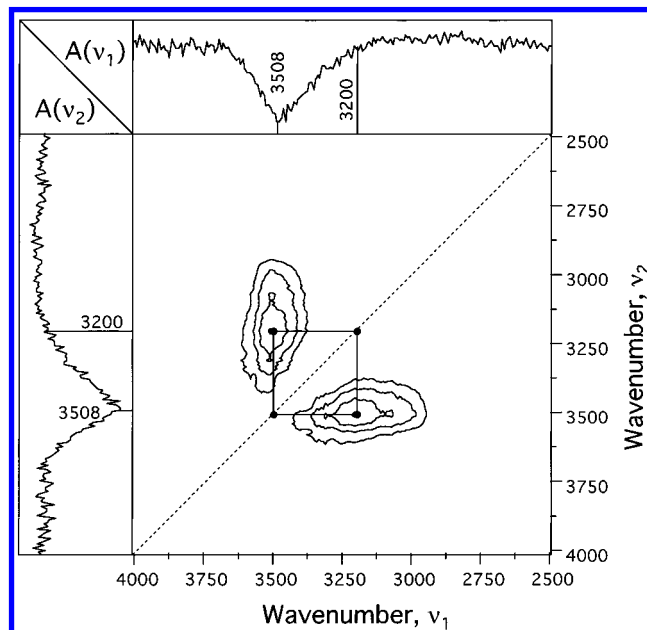


**Figure 7.** Asynchronous 2D IR spectrum constructed from the 1D spectra collected in the potential range between 0 and 0.8 V in Figure 3.

The structure of the icelike water layer on metal surfaces has been extensively studied in UHV by means of several modern surface analytical techniques.<sup>10</sup> The proposed icelike structure is essentially equivalent to the basal plane of ice  $I_h$  in contact with the surface (Figure 5c). Water molecules in the first layer adjacent to the surface are oriented with hydrogen ends directing slightly toward the solution phase and are hydrogen bonded to the molecules in the second layer. This icelike structure model is suitable to explain the observed IR spectra. Note that the molecular axis of each water molecule in the first layer is inclined by about  $60^\circ$  from the surface normal, which explains the weak absorption of both  $\nu(\text{OH})$  and  $\delta(\text{HOH})$



modes. If water molecules were oriented with their dipoles normal to the surface directing the hydrogen ends toward the surface as assumed in classical double-layer models,<sup>2</sup> the water bands should be observed strongly.

At potentials around and below the pzc, the water spectra acquired in the sulfuric acid solution are essentially identical with those acquired in perchloric acid solutions.<sup>13</sup> The broad  $\nu(\text{OH})$  band of the icelike water layer has been observed in perchloric acid solutions also. The experimental results obtained at potentials around and below the pzc are in good agreement with the predictions made by molecular dynamics simulations.<sup>23–25</sup> However, specific anion adsorption is not taken into account in the molecular dynamics simulations. A strong anion dependence is seen in the high potential range where anion adsorption encounters. The adsorption of hydrophobic anions, such as perchlorate and chloride anions, partly brakes hydrogen bonds in the icelike water layer, yielding an additional sharp  $\nu(\text{OH})$  band around  $3600\text{ cm}^{-1}$  characteristic for a non-hydrogen bonded OH moiety.<sup>13</sup> Such sharp  $\nu(\text{OH})$  band is not observed in the sulfuric acid solution, suggesting that sulfate anion is adsorbed on the electrode surface by forming strong hydrogen bonds with surrounding water molecules. In Figure 6, a shoulder around  $3400\text{ cm}^{-1}$  is seen to increase in intensity as the potential is made more positive (namely, as the sulfate coverage increases). We assign this band to water molecules hydrogen bonded to adsorbed sulfate anions.

At more positive potentials than  $0.75\text{ V}$ , the  $\nu(\text{OH})$  and  $\delta(\text{HOH})$  bands abruptly increase in intensity (Figure 3). Since the number of water molecules at the interface decreases as the fractional coverage of sulfate increases, the growth of the water bands is interpreted as that the water dipole becomes more oriented along the surface normal. During this course, the  $\nu(\text{OH})$  band shifts to higher wavenumbers (from  $3240\text{ cm}^{-1}$  at  $0.77\text{ V}$  to  $3480\text{ cm}^{-1}$  at  $1.0\text{ V}$ ). The upshift indicates the weakening of the sulfate–water hydrogen bonding. The spectral changes terminate at about  $1.0\text{ V}$  and both the intensities and peak positions are unaltered at more positive potentials.

**Adsorption of Sulfate Anion.** Infrared RAS studies of anion adsorption on polycrystalline and (111) single-crystal Au surfaces in sulfuric acid solutions have been reported in the literature.<sup>6,27,28</sup> The reported spectra are different from each other. The spectrum of the adsorbed anion obtained in the present study by using the ATR-SEIRAS technique is essentially identical to the RA spectra obtained by Edens et al.<sup>6</sup> by means of a well-defined (111) single-crystal electrode. The integrated intensity of the sulfate band is plotted in Figure 8a (circles) as a function of the potential. The intensity vs potential curve is well correlated with the Gibbs excess of sulfate on Au-(111) determined by means of chronocoulometric and radiotracer methods.<sup>9</sup>

The sulfate band shifts to higher wavenumbers with increasing the potential, as plotted in Figure 8b (circles). The peak position plot displays two inflections at about  $0.75$  and  $1.0\text{ V}$ . The shift is about  $30\text{ cm}^{-1}/\text{V}$  at potentials below  $0.75\text{ V}$ ,  $100\text{ cm}^{-1}/\text{V}$  at  $0.75$ – $1.0\text{ V}$ , and  $60\text{ cm}^{-1}/\text{V}$  at potentials above  $1.0\text{ V}$ . The inflection around  $1.0\text{ V}$  has already been reported by Edens et al.<sup>6</sup> Two possible mechanisms have been proposed to explain the potential-dependent peak shift of the  $\nu(\text{SO})$  mode: Stark tuning

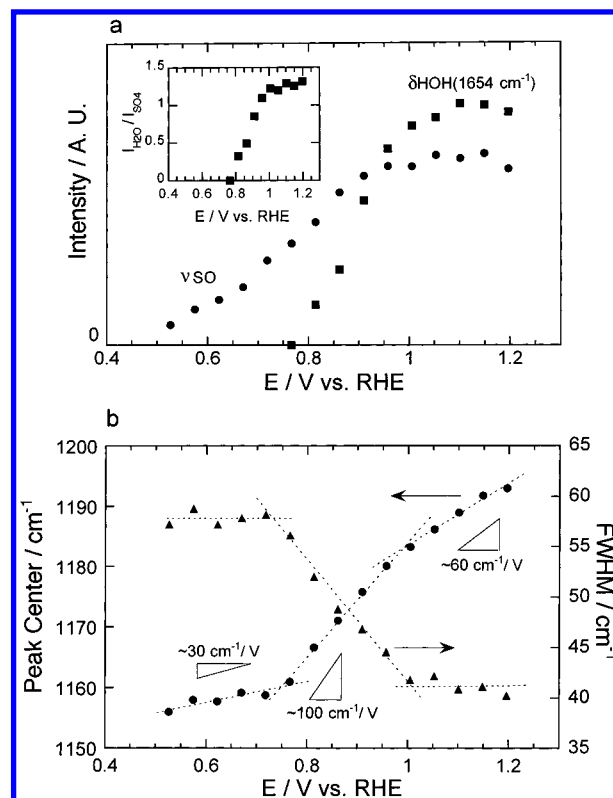


**Figure 8.** Plots of (a) the integrated band intensities of the  $\nu(\text{SO})$  mode of sulfate (circles) and  $\delta(\text{HOH})$  mode of water (squares), and (b) the peak position (circles) and half-width (triangles) of the  $\nu(\text{SO})$  band, as a function of the applied potential. The inset in (a) shows the intensity ratio between the water and sulfate bands as a function of the applied potential. The dashed lines are to guide the eye.

and electron back-donation mechanisms.<sup>29</sup> The back-donation of electron from the metal to empty orbitals of adsorbed sulfate has been confirmed by core electron energy loss spectroscopy.<sup>30</sup> However, these two mechanisms do not explain the inflections in the peak position vs potential plot. The inflections are ascribed to the change in the vibrational properties of sulfate, which are clearly seen from the half-width vs potential plot shown in the same figure (triangles). With increasing the potential, the width decreases from about  $60\text{ cm}^{-1}$  at  $0.75\text{ V}$  to about  $40\text{ cm}^{-1}$  at  $1.0\text{ V}$ , indicating that adsorbate–adsorbate and/or adsorbate–metal interactions become more uniform with increasing the potential.<sup>31</sup> It is noteworthy that the spectral changes of sulfate in the potential range between  $0.75$  and  $1.0\text{ V}$  are well correlated with those of water molecules hydrogen-bonded to sulfate. The water bands at  $1654$  and  $3420$ – $3480\text{ cm}^{-1}$  start to grow at about  $0.75\text{ V}$ , where the width of the sulfate band starts to decrease (Figure 8). At a potential where the intensity of the water bands saturates, the width of sulfate band becomes constant (about  $1.0\text{ V}$ ). No spectral changes are seen for both water and sulfate above  $1.0\text{ V}$  except for the moderate upshift of the sulfate band by Stark tuning and/or back-donation mechanisms. The intensity ratio of the water and sulfate bands is constant in the high potential range (inset in Figure 8a). These results strongly suggest

(27) Parry, D. B.; Samant, M. G.; Seki, H.; Philpott, M. R.; Ashley, K. *Langmuir* **1993**, *9*, 1978.

(28) Weber, W.; Nart, F. C. *Langmuir* **1996**, *12*, 1895.

(29) Faguy, P. W.; Markovic, N.; Adzic, R. R.; Fierro, C. A.; Yeager, E. B. *J. Electroanal. Chem.* **1990**, *289*, 245.

(30) Mrozek, P.; Han, M.; Sung, Y.-E.; Wieckowski, A. *Surf. Sci.* **1994**, *319*, 21.

(31) Hoffmann, F. M. *Surf. Sci. Rep.* **1983**, *3*, 107.

that the sulfate–water hydrogen bonding is responsible for the change in the  $\nu(\text{SO})$  vibration. As mentioned above, the  $\nu(\text{OH})$  band upshifts (namely, the hydrogen-bonding becomes weaker) in this potential range. The weakening of the hydrogen-bonding should result in the upshift of the  $\nu(\text{SO})$  band. Thus, the  $\nu(\text{SO})$  band shows a larger peak shift in this potential range than in lower and higher potential ranges.

The width vs potential plot in Figure 8b strongly suggests that adsorbed sulfate anions start to form short-ranged domains around 0.75 V and a long-ranged ordered adlayer is formed around 1.0 V. The potential at which the ordered adlayer is believed to be formed is 0.1 V negative to the disorder–order transition potential signaled by the sharp current spike (1.1 V). This discrepancy probably arises from defects on the surface.<sup>21</sup> The formation of sulfate domains at lower potentials than the disorder–order transition potential has been suggested by Magnussen et al.<sup>5</sup> They showed that the phase transition occurs via an island-growth mechanism. In other STM studies of the (111) surfaces of Au, Rh, and Pt in sulfuric acid solutions,<sup>6–8</sup> no sulfate domains have been observed at potentials negative to the phase transition potential. The domains may be mobile or unstable in the time scale of STM measurements; thus they are hardly visible to STM.

**Adsorbed Geometry of Sulfate.** Efforts to determine the adsorption site and geometry of sulfate have been made by using STM, but the results are controversial. Adsorption at bridge sites via two oxygen atoms,<sup>5</sup> at atop sites,<sup>6</sup> and at 3-fold hollow sites via three oxygen atoms<sup>7,8</sup> were deduced.

Infrared spectra have information on the adsorbed geometry. This issue has been discussed by Nart et al.,<sup>28,32</sup> but a clear conclusion has not yet been reached. The  $T_d$  symmetry of free sulfate anion is reduced to  $C_{3v}$ ,  $C_{2v}$ , or lower depending upon coordination geometry. Due to the symmetry reduction, the triply degenerate  $\nu(\text{SO})$  mode ( $\nu_3$ ) of the free anion (at 1105  $\text{cm}^{-1}$  in bulk solutions) splits into two modes (for  $C_{3v}$  symmetry) or three modes (for  $C_{2v}$  and lower symmetries). Among these modes only one symmetric  $\nu(\text{SO})$  mode ( $\nu_3'$ ) is allowed in the surface spectrum both for  $C_{3v}$  and  $C_{2v}$  symmetries due to the surface selection rule. The observation of only one sulfate band above 1000  $\text{cm}^{-1}$  argues that the adsorbed sulfate has  $C_{3v}$  or  $C_{2v}$  symmetry. The IR-inactive totally symmetric  $\nu(\text{SO})$  ( $\nu_1$ ) mode of the free anion (983  $\text{cm}^{-1}$ ) also becomes active upon adsorption. Since this mode should shift to lower frequencies by the coordination to metal atoms,<sup>33</sup> the 955  $\text{cm}^{-1}$  band observed by Edens et al.<sup>6</sup> and Weber and Nart<sup>28</sup> (and also in the present study, Figure 9) is assigned to the  $\nu_1$  mode.

Several infrared spectra of metal–sulfate complexes have been reported in the literature.<sup>22</sup> Comparison of the surface spectra with the existing spectral data of sulfato complexes is informative in considering the coordination geometry. Unidentate complexes (sulfate coordinated to one metal atom via one oxygen atom) show the  $\nu_3'$  mode at 1030–1060  $\text{cm}^{-1}$ . Bridged bidentate complexes (sulfate coordinated to two metal atoms via two oxygen atoms) show this mode at a slightly higher range of 1090–1110  $\text{cm}^{-1}$ . Chelating bidentate complexes (sulfate coordinated to one metal atom via two oxygen atoms) shows the  $\nu_3'$  modes at 1125–1170  $\text{cm}^{-1}$ .<sup>22</sup> The upshift of the  $\nu_3'$  mode

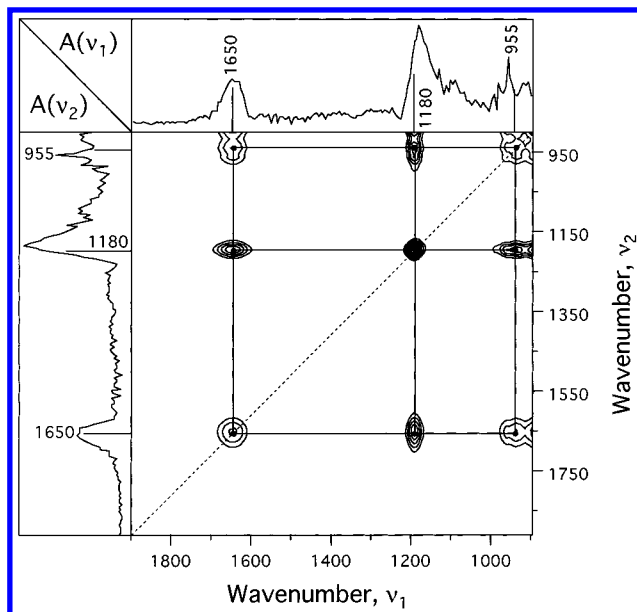


**Figure 9.** Synchronous 2D IR spectrum constructed from the 1D spectra collected in the potential range between 0.8 and 1.2 V in Figure 3.

with increasing the coordination number is explained by the increase of the force constant of the S–O (of uncoordinated oxygen) bond.<sup>33–35</sup> Since the S–O stretch dominantly contributes to the  $\nu_3'$  mode rather than the S–O\* (of coordinated oxygen) stretch,<sup>33</sup> the increase in the S–O bond order results in the upshift of the  $\nu_3'$  mode. Unfortunately, no spectral data are available for complexes in which sulfate is coordinated to metal atoms via three oxygens. Nevertheless, it is reasonably assumed in this context that the  $\nu_3'$  mode shifts to higher than 1100  $\text{cm}^{-1}$  if sulfate is coordinated to three metal atoms via three oxygen atoms. If sulfate is coordinated to one metal atom via three oxygen atoms, this mode will be observed at a wavenumber higher than 1125–1170  $\text{cm}^{-1}$ .

The frequency of the  $\nu_3'$  mode for sulfate anion adsorbed on the electrode surface is located around 1155  $\text{cm}^{-1}$  at potentials close to the pzc where the peak shift caused by Stark tuning and back-donation mechanisms will be small or negligible. This frequency is higher than that of the  $\nu_3'$  modes for unidentate and bidentate sulfato complexes and is in the frequency region for chelating bidentate complexes. However, chelating bidentate adsorption at atop sites cannot explain the electrochemical measurements that sulfate is adsorbed strongly on Au(111), less strongly on (110), and very little or not at all on (100).<sup>18,19</sup> Therefore, sulfate anion is the most likely to be adsorbed via three oxygen atoms at a 3-fold hollow site, yielding  $C_{3v}$  symmetry.

**Water–Sulfate Coadsorbed Structure.** The ordered ( $\sqrt{3} \times \sqrt{7}$ ) sulfate adstructure on Au(111) is rearranged to a ( $\sqrt{3} \times \sqrt{3}$ )R30° adstructure when the electrode is emerged from sulfuric acid solutions to UHV.<sup>30</sup> A plausible explanation for the more open adstructure formed in solutions is that coadsorption of water species within the sulfate adlayer prevents the close contact adsorption of sulfate anions. Possible species incorporated in the sulfate adlayer are hydronium cation<sup>6</sup> and water molecule.<sup>7,8</sup>

We have described above that hydronium cation is adsorbed on the electrode surface at potentials negative of the pzc. However, hydronium cation is not adsorbed

(32) Nart, F. C.; Iwasita, T. *J. Electroanal. Chem.* **1992**, 322, 289–300.

(33) Tanaka, N.; Sugi, H.; Fujita, J. *Bull. Chem. Soc. Jpn.* **1964**, 37, 640.

(34) Thewalt, U. *Acta Crystallogr.* **1971**, B27, 1744.

(35) Cotton, F. A.; Falvello, L. R.; Han, S. *Inorg. Chem.* **1982**, 21, 2889.

at the high potential range where sulfate anion is adsorbed, which is seen very clearly in the synchronous 2D spectrum shown in Figure 9 constructed from the spectra collected between 0.8 and 1.2 V in Figure 3. If hydronium cations were coadsorbed with sulfate anions, hydronium bands should increase in intensity as the sulfate coverage increases, and cross peaks should be observed between the hydronium bands and sulfate bands in the synchronous 2D spectrum. However, no cross peaks appear at the frequencies of hydronium bands. The band which synchronously changes in intensity with the sulfate band at  $1180\text{ cm}^{-1}$  is the  $1654\text{ cm}^{-1}$  band of water,<sup>36</sup> indicating that a water molecule rather than hydronium cation is incorporated in the sulfate adlayer. Shi et al.<sup>9</sup> proposed that hydronium cations are present in the diffusion part of the double-layer only. The IR data do not conflict with this proposal because ATR-SEIRAS probes only the very near vicinity of the electrode surface.

The synchronous 2D spectrum also shows the presence of a band at  $955\text{ cm}^{-1}$ , which changes its intensity synchronously with the sulfate band at  $1180\text{ cm}^{-1}$ . This band is undoubtedly assigned to the totally symmetric  $\nu_1$  mode of adsorbed sulfate. The low-frequency region was included in the 2D correlation analysis in order to show that this technique is very useful to detect weak absorption bands even if they are buried in strong background and noise signals.

The icelike water layer on (111) metal surfaces has a  $(\sqrt{3} \times \sqrt{3})R30^\circ$  structure and water molecules in the first layer are located at atop sites.<sup>10</sup> If sulfate anions are adsorbed at 3-fold hollow sites with locating oxygen atoms at atop sites, the sulfate adsorption will not greatly disturb the icelike water structure. On the basis of this idea, Wan et al.<sup>7</sup> proposed that an icelike water layer is incorporated within the  $(\sqrt{3} \times \sqrt{7})$  ordered sulfate adlayer on Ru(111). In fact, the adsorption of sulfate does not disturb the icelike water layer when sulfate coverage is small (in the potential range below 0.75 V) as shown in Figure 6. The IR data in turn may suggest the sulfate adsorption at 3-fold hollow sites. When sulfate coverage reaches to about half of full coverage (at about 0.75 V), however, adsorbed sulfate anions start to form domains and greatly change the water layer structure (Figure 8).

To explain the change of the interfacial structure at high sulfate coverage, we propose a model that water molecules bridge two adjacent sulfate anions via hydrogen-bonding as illustrated in Figure 5d. This model is based on the following two findings. One is that the frequency of the  $\delta(\text{HOH})$  band observed in the potential range above 0.75 V ( $1654\text{ cm}^{-1}$ ) is higher than that in the bulk ( $1643\text{ cm}^{-1}$ ) by  $11\text{ cm}^{-1}$ . As mentioned above, the sulfate–water hydrogen bonding becomes weaker as the potential increases judging from the upshift of the  $\nu(\text{OH})$  band. Generally the  $\delta(\text{HOH})$  band should shift to lower frequencies as hydrogen bonding becomes weaker, but the result is reverse. The upshift of the  $\delta(\text{HOH})$  mode is unusual and is noteworthy. The large strain on the  $\delta(\text{HOH})$  mode suggests that both hydrogen ends of each water molecule are spatially fixed. The other is that the intensity ratio of the water and sulfate bands is constant at potentials above 1.0 V (inset in Figure 8a), which suggests the formation of a sulfate–water pair. On the basis of the IR and Raman studies of various forms of

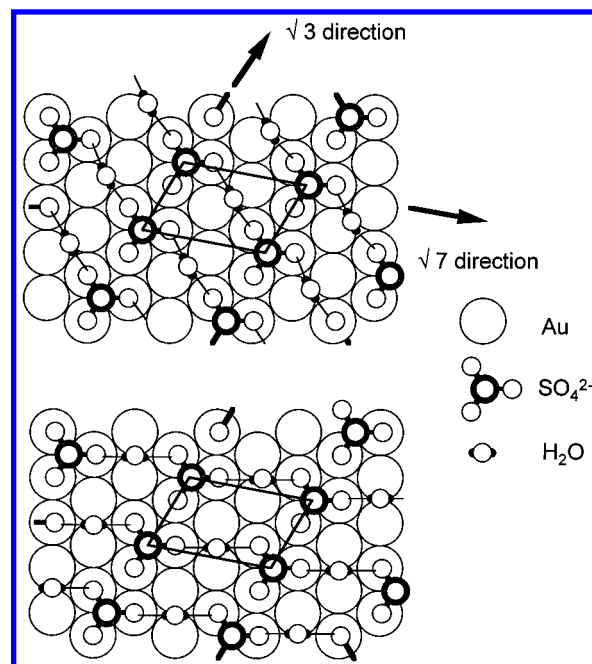


**Figure 10.** Two possible positions for water molecules incorporated in the ordered  $(\sqrt{3} \times \sqrt{7})$  sulfate adlayer. Water molecules bridge coordinated sulfate oxygen atoms via hydrogen bonding. Water molecules that bridge uncoordinated sulfate oxygen atoms are omitted for clarity.

ice,<sup>37</sup> the O–O separation in the hydrogen-bonded system is estimated to be about 0.3 nm from the  $\nu(\text{OH})$  frequency of  $3480\text{ cm}^{-1}$ . If the HOH bond angle is assumed to be  $104.5^\circ$  as in the gas phase, a water molecule can bridge two hydrogen acceptors separated by 0.47 nm. This value is close to the possible nearest neighbor distance between two adsorbed sulfate anions on the Au(111) surface ( $\sqrt{3}a_0 = 0.5\text{ nm}$ , where  $a_0$  is the nearest neighbor distance between surface atoms, see Figure 10). Therefore, it is believed that water molecules can bridge uncoordinated oxygen atoms of sulfate anions adsorbed at the nearest neighbor positions (Figure 5d, left). Although the distance between the centers of the anions adsorbed at the second nearest neighbor sites is  $\sqrt{7}a_0 = 0.76\text{ nm}$ , the closest distance between coordinated oxygen atoms of the sulfate anions is also 0.5 nm. Hence bridging hydrogen bonding between them (Figure 5d, right) will also be possible.

The possibility that water molecules bridge adjacent sulfate anions becomes larger as sulfate coverage increases (namely, the distance between sulfate anions is reduced), which accounts for the remarkable spectral changes of both water and sulfate at relatively high sulfate coverages (at high potentials). The electrosorption valency for sulfate adsorbed on Au(111) is between 0.7 and 1.0, and the adsorbed anion has negative charge.<sup>38</sup> Bridging hydrogen bonding will diminish the Coulombic repulsions between adjacent sulfate anions. In particular, water molecules that bridge coordinated oxygen atoms of the anions are located between them and will effectively screen the Coulombic repulsions. Therefore bridging hydrogen bonding is believed to facilitate the formation of sulfate domains.

This model is suitable to explain the weak tunneling spots seen in the STM images of the well-ordered  $(\sqrt{3} \times \sqrt{7})$  sulfate adstructure on (111) surfaces formed at high

(36) The positions of cross peaks do not necessarily represent actual frequencies of the bands, since they are determined by the net phase angles of dynamic signals at any given wavenumbers. The discrepancy becomes larger when the peak frequency shifts with potential.

(37) Kamb, B. In *Structural Chemistry and Molecular Biology*; Rich, A., Davidson, N., Eds.; Freeman: San Francisco, CA, 1968; p 507.

(38) Shi, Z.; Lipkowski, J.; Mirwald, S.; Pettinger, B. *J. Electroanal. Chem.* **1995**, *396*, 115.



potentials. It has been reported that the weak tunneling spots appear either near the center of the unit cell or at a position between main bright spots along the  $\sqrt{7}$  direction, depending upon imaging conditions.<sup>5-8</sup> For the  $(\sqrt{3} \times \sqrt{7})$  sulfate adstructure model by Wan et al.<sup>7</sup> and Funtikov et al.,<sup>8</sup> two positions are considerable for the water molecules bridging coordinated sulfate oxygen atoms as illustrated in Figure 10: near the center of the unit cell (a) and a position between sulfate anions along the  $\sqrt{7}$  direction (b). The nearest and the third nearest neighbor O-O distances of sulfate anions ( $a_0$  and  $2a_0$ ) are too small and too large, respectively, to form bridging hydrogen bonds. Since the water molecules are not directly bonded to the surface metal atoms, they are not necessarily located at atop sites or other special sites of the underlying (111) surface, and our model can be incorporated in the sulfate adstructure model by Edens et al.<sup>6</sup> in which sulfate anions are located at atop sites. Therefore, we assign the weak tunneling spots in the reported STM images to water molecules. The two possible positions for the water molecules may explain the uncertainty of the positions of the weak tunneling spots.

Finally, a very important question is why adsorbed sulfate anions form the  $(\sqrt{3} \times \sqrt{7})$  ordered structure in solutions rather than more uniformly ordered structures such as  $(\sqrt{3} \times \sqrt{3})$  and  $(\sqrt{7} \times \sqrt{7})$ . In our model, bridging hydrogen bonds that connect uncoordinated sulfate oxygen atoms facilitate the sulfate adsorption at the closest sites separated by  $\sqrt{3}a_0$ , whereas bridging hydrogen bonds that connect coordinated sulfate oxygen atoms facilitate the sulfate adsorption at the second closest sites separated by  $\sqrt{7}a_0$ . The two different bridging hydrogen bonds will play a role in the  $(\sqrt{3} \times \sqrt{7})$  ordered structure formation.

### Conclusion

The spectrum of water on a Au(111) electrode surface changes in both intensity and frequency as the potential changes, which are interpreted in terms of the potential-

dependent reorientation of the molecules in the first layer adjacent to the surface. The water dipole is slightly directing toward the surface at potentials negative of the pzc and is parallel to the surface around the pzc. At potentials slightly positive of the pzc, the water dipole reorients slightly toward the solution phase and an icelike structure is formed via hydrogen bonding with water molecules in the second layer. The orientations deduced from the IR data obtained at the low potentials where sulfate adsorption is negligible are in good agreement with the predictions made by molecular dynamics simulations.

Sulfate anion is adsorbed at the 3-fold hollow sites of the Au(111) surface via three oxygen atoms. At potentials slightly above the pzc, the sulfate adsorption does not greatly disturb the icelike water layer. As the potential increases and the coverage of sulfate increases to about half of full coverage, sulfate anions start to form domains and the well-ordered  $(\sqrt{3} \times \sqrt{7})$  sulfate adstructure is formed around a potential where sulfate coverage saturates. Water molecules are incorporated in the sulfate adlayer and bridge neighboring sulfate anions by forming hydrogen bonds between uncoordinated sulfate oxygens and between coordinated sulfate oxygens. The bridging hydrogen bonds facilitate the sulfate adsorption at sites separated by  $\sqrt{3}a_0$  and  $\sqrt{7}a_0$ , which may play a role in forming the  $(\sqrt{3} \times \sqrt{7})$  sulfate adstructure. The weak tunneling spots seen in the previously reported STM images of the ordered sulfate adlayer are attributed to water molecules bridging the coordinated oxygens of neighboring sulfate anions.

**Acknowledgment.** This work was supported by Grant-in-Aid for Scientific Research on Priority Area Research (Nos. 09237101, 09218204, 09241201), for Scientific Research (B) (No. 08454171), and for COE Research from Ministry of Education, Science, Sports and Culture, Japan.

LA971110V